





Impact of Mutations at Arg220 and Thr237 in PER-2 β -Lactamase on Conformation, Activity, and Susceptibility to Inhibitors

Melina Ruggiero,^{a,b} Lucrecia Curto,^{c,d} Florencia Brunetti,^a  Eric Sauvage,^e Moreno Galleni,^e  Pablo Power,^{a,b} Gabriel Gutkind^{a,b}

Universidad de Buenos Aires, Facultad de Farmacia y Bioquímica, Departamento de Microbiología, Inmunología y Biotecnología, Cátedra de Microbiología, Buenos Aires, Argentina^a; Consejo Nacional de Investigaciones Científicas y Técnicas (CONICET), Buenos Aires, Argentina^b; Universidad de Buenos Aires, Facultad de Farmacia y Bioquímica, Departamento de Química Biológica, Buenos Aires, Argentina^c; Consejo Nacional de Investigaciones Científicas y Técnicas (CONICET), Instituto de Química y Fisicoquímica Biológicas (IQUIFIB), Buenos Aires, Argentina^d; InBioS, Centre d'Ingénierie des Protéines, Université de Liège, Liège, Belgium^e

ABSTRACT PER-2 accounts for up to 10% of oxyimino-cephalosporin resistance in *Klebsiella pneumoniae* and *Escherichia coli* in Argentina and hydrolyzes both cefotaxime and ceftazidime with high catalytic efficiencies (k_{cat}/K_m). Through crystallographic analyses, we recently proposed the existence of a hydrogen bond network connecting Ser70-Gln69-oxyanion water-Thr237-Arg220 that might be important for the activity and inhibition of the enzyme. Mutations at Arg244 in most class A β -lactamases (such as TEM and SHV) reduce susceptibility to mechanism-based inactivators, and Arg220 in PER β -lactamases is equivalent to Arg244. Alterations in the hydrogen bond network of the active site in PER-2, through modifications in key residues such as Arg220 and (to a much lesser extent) Thr237, dramatically impact the overall susceptibility to inactivation, with up to ~300- and 500-fold reductions in the rate constant of inactivation (k_{inact}/K_i values for clavulanic acid and tazobactam, respectively). Hydrolysis on cephalosporins and aztreonam was also affected, although to different extents compared to with wild-type PER-2; for cefepime, only an Arg220Gly mutation resulted in a strong reduction in the catalytic efficiency. Mutations at Arg220 entail modifications in the catalytic activity of PER-2 and probably local perturbations in the protein, but not global conformational changes. Therefore, the apparent structural stability of the mutants suggests that these enzymes could be possibly selected *in vivo*.

KEYWORDS Arg220, ESBL, Thr237, cefotaximase, ceftazidimase, inhibitor resistant, mechanism-based inhibitor

Since the description of the first two acquired narrow-spectrum β -lactamases (TEM-1, and SHV-1), clinically relevant β -lactamases evolved following two main paths, contributing to the alarming resistance levels found today (1). One of them involves accumulation of few mutations in key positions directly affecting the enzyme's activity (or inhibition) profile. By this mechanism, some β -lactamases evolved from a broad- to an extended-spectrum profile, resulting in enzymes like the first known extended-spectrum β -lactamases (ESBLs) and inhibitor-resistant (IR) enzymes (2–5). The second path is relevant for some ESBLs and involves direct dissemination of originally chromosomal genes residing in environmental or nonpathogenic species to pathogens (6, 7).

Received 11 October 2016 Returned for modification 11 November 2016 Accepted 14 March 2017

Accepted manuscript posted online 20 March 2017

Citation Ruggiero M, Curto L, Brunetti F, Sauvage E, Galleni M, Power P, Gutkind G. 2017. Impact of mutations at Arg220 and Thr237 in PER-2 β -lactamase on conformation, activity, and susceptibility to inhibitors. *Antimicrob Agents Chemother* 61:e02193-16. <https://doi.org/10.1128/AAC.02193-16>.

Copyright © 2017 American Society for Microbiology. All Rights Reserved.

Address correspondence to Pablo Power, ppower@ffyb.uba.ar, or Gabriel Gutkind, ggutkind@ffyb.uba.ar.

TABLE 1 Inhibition parameters of PER-2 and derived Arg220 and Thr237 mutants

PER-2	Clavulanic acid				Tazobactam			
	k_{inact} (s^{-1})	K_i (μM)	k_{inact}/K_i ($\mu\text{M}^{-1} \text{s}^{-1}$)	Relative k_{inact}/K_i (%) ^a	k_{inact} (s^{-1})	K_i (μM)	k_{inact}/K_i ($\mu\text{M}^{-1} \text{s}^{-1}$)	Relative k_{inact}/K_i (%) ^a
Wild type	0.031 ± 0.001	0.064 ± 0.007	0.48 ± 0.07	100	0.047 ± 0.002	0.18 ± 0.02	0.26 ± 0.04	100
Mutant								
Arg220Leu	0.045 ± 0.001	4.1 ± 0.2	0.0109 ± 0.0008	2.3	0.016 ± 0.001	10 ± 1	0.0016 ± 0.0004	0.6
Arg220Ser	0.055 ± 0.002	1.8 ± 0.1	0.031 ± 0.003	6.5	0.0172 ± 0.0005	2.8 ± 0.2	0.0062 ± 0.0007	2.4
Arg220Gly	0.11 ± 0.01	80 ± 10	0.0014 ± 0.0003	0.3	0.0157 ± 0.0006	31 ± 3	0.00050 ± 0.00007	0.2
Arg220His	0.032 ± 0.002	3.3 ± 0.5	0.010 ± 0.002	2.0	0.0150 ± 0.0005	5.1 ± 0.6	0.0029 ± 0.0004	1.1
Arg220Thr	ND ^b	ND	0.0068 ± 0.0002	1.4	0.022 ± 0.001	11 ± 1	0.0019 ± 0.0004	0.7
Arg220Cys	0.31 ± 0.04	19 ± 3	0.016 ± 0.005	3.3	0.0187 ± 0.0004	6.0 ± 0.4	0.0031 ± 0.0002	1.2
Thr237Ala	0.027 ± 0.001	0.070 ± 0.009	0.38 ± 0.07	79.8	0.022 ± 0.002	0.27 ± 0.06	0.08 ± 0.02	30.6

^aRelative to wild-type PER-2.^bND, not determined.

Plasmid-borne PER (i.e., “*Pseudomonas* extended resistance”) extended-spectrum β -lactamases (8) have been detected in few locations around the world. In South American countries like Argentina and Uruguay, PER-2 is still the only variant detected and may account for up to 10% and 5% of oxyimino-cephalosporin resistance in *Klebsiella pneumoniae* and *Escherichia coli*, respectively (1, 9, 10), as the second most prevalent ESBL family after the pandemic CTX-M derivatives. PER-2 has 86% amino acid sequence identity with PER-1. Both hydrolyze oxyimino-cephalosporins with high catalytic efficiencies (k_{cat}/K_m) for cefotaxime and ceftazidime, even if PER-2 is ca. 20-fold more efficient than PER-1 on the latter; they are also strongly inhibited by mechanism-based inhibitors such as clavulanate and tazobactam (11, 12).

Recently, we solved the crystallographic structure of PER-2 at 2.2 Å (13). Compared to other class A β -lactamases, PER-2 has an inverted Ω loop due to a *trans* bond between residues 166 and 167 and an expanded β 3- β 4 loop, creating an enlarged active site cavity that allows for efficient oxyimino-cephalosporin hydrolysis. We also provided structural evidence for the existence of a hydrogen bond network connecting Ser70-Gln69-oxyanion water-Thr237-Arg220 that might be important for the activity and inhibition of the enzyme (13).

It has been hypothesized that mutations in either Arg220 (the counterpart of Arg244 in TEM/SHV variants) or Thr237 would probably result in modifications in kinetic behavior; the same role has also been suggested for Arg220 in PER-1 and other β -lactamases with an arginine at this position, such as KPC-2 (12–14). It is noteworthy that Arg220 in PER β -lactamases is replaced by Arg276 in the CTX-M enzymes (15) and Arg244 in most of the other class A β -lactamases, especially TEM and SHV. Nevertheless, only mutations at Arg244 have proven to negatively impact inhibition by mechanism-based inactivators, selecting “inhibitor-resistant” β -lactamases (16–18). It is noteworthy in all of these arginine residues that the positively charged guanidinium group shares the same spatial position in the structure.

As no variants of PER β -lactamases with decreased susceptibility to mechanism-based inhibitors have been described among clinical isolates so far, the rationale of this study was to evaluate if mutations at Arg220 and Thr237 in PER-2 β -lactamase are able to modify the response to mechanism-based inhibitors and their impact on the activity toward different substrates, so as to anticipate their possible *in vivo* selection.

RESULTS AND DISCUSSION

Mutations at Arg220 and Thr237 have different effects on the inhibition efficiency of mechanism-based inhibitors. Mutations at Arg220 resulted in a marked increase in the K_i values for the inhibitors, which led to a dramatic decrease in the inactivation efficiencies (expressed as the rate constant of inactivation [k_{inact}/K_i] (Table 1). In the Arg220Gly variant, this resulted in ~300- and 500-fold reductions in the k_{inact}/K_i values for clavulanic acid and tazobactam, respectively. In other mutants,

TABLE 2 Steady-state kinetic parameters of PER-2 and derived Arg220 and Thr237 mutants

	Ampicillin			Cephalothin			Cefotaxime		
	k_{cat} (s^{-1})	K_m (μM)	k_{cat}/K_m ($\mu M^{-1} s^{-1}$)	k_{cat} (s^{-1})	K_m (μM)	k_{cat}/K_m ($\mu M^{-1} s^{-1}$)	k_{cat} (s^{-1})	K_m (μM)	k_{cat}/K_m ($\mu M^{-1} s^{-1}$)
PER-2									
Wild type	53.0 \pm 0.5	18 \pm 1	3.0 \pm 0.2	49.0 \pm 0.8	12.7 \pm 0.7	3.9 \pm 0.3	92 \pm 3	51 \pm 3	1.8 \pm 0.1
Mutant									
Arg220Leu	105 \pm 3	108 \pm 10	1.0 \pm 0.1	27.8 \pm 0.8	58 \pm 3	0.48 \pm 0.04	12.3 \pm 0.6	129 \pm 11	0.10 \pm 0.01
Arg220Ser	72 \pm 2	81 \pm 8	0.9 \pm 0.1	22.6 \pm 0.5	43 \pm 2	0.53 \pm 0.04	21.0 \pm 0.9	118 \pm 9	0.18 \pm 0.02
Arg220Gly	64 \pm 1	125 \pm 5	0.51 \pm 0.03	20.4 \pm 0.5	510 \pm 22	0.040 \pm 0.003	9.2 \pm 0.6	543 \pm 49	0.017 \pm 0.003
Arg220His	72 \pm 2	60 \pm 6	1.2 \pm 0.1	14.2 \pm 0.4	82 \pm 5	0.17 \pm 0.01	32 \pm 1	263 \pm 26	0.12 \pm 0.02
Arg220Thr	100 \pm 3	86 \pm 8	1.2 \pm 0.2	31 \pm 1	63 \pm 4	0.50 \pm 0.05	13.3 \pm 0.3	104 \pm 5	0.13 \pm 0.01
Arg220Cys	124 \pm 3	62 \pm 6	2.0 \pm 0.2	17.5 \pm 0.5	40 \pm 3	0.44 \pm 0.05	21.2 \pm 0.9	139 \pm 11	0.15 \pm 0.02
Thr237Ala	133 \pm 3	30 \pm 3	4.4 \pm 0.6	13.6 \pm 0.4	6.8 \pm 0.8	2.0 \pm 0.3	9.9 \pm 0.2	13.1 \pm 0.7	0.76 \pm 0.06

^a K_m determined as K_i .

^bND, not determined.

maximums of 6.5% and 2.4% relative k_{inact}/K_i values (both values corresponding to the Arg220Ser mutant) were observed for clavulanic acid and tazobactam, respectively, compared to wild-type PER-2, which clearly indicates that the substitution of this arginine residue at position 220 leads to major impact in the inhibition efficiency of mechanism-based inhibitors. These results reinforce the previous hypothesis about the essential role of Arg220 in the activity of PER-2 (13).

This behavior suggests that mutations at Arg220, resulting in a modification or suppression of the positive charge conferred by the arginine residue, entail a negative impact in the accommodation of the inhibitor within the active site and the proper formation of the Michaelis complex. These changes are expected to have different consequences in the hydrogen bond network integrity, depending on the specific amino acid that replaces the arginine residue. In fact, substitution for Arg220 by lysine in KPC-2 has been demonstrated to result in an "inhibitor-susceptible" variant (probably by reinforcing the positive environment), while the Arg220Met mutation reduced the inhibition efficiency on KPC-2 (14).

As shown in Table 1, the Thr237Ala mutation resulted in only minor (but still detectable) differences in inhibition by both inhibitors compared with wild-type PER-2.

Hydrolysis of several β -lactams is also affected by mutations at Arg220 and Thr237. Modifications in Arg220 of PER-2 not only affect the susceptibility to inhibitors but also seem to have an impact on the catalytic behavior toward several antibiotics, as observed in Table 2. For all of the Arg220 mutants, the K_m values toward ampicillin were reduced up to 7-fold, the K_m for the Arg220Gly variant being the most affected. In some cases, the k_{cat} constants somewhat compensated this decrease in the affinity, resulting in k_{cat}/K_m values of ampicillin that were almost invariable for some mutants, except for Arg220Gly. The Thr237Ala mutation resulted in higher k_{cat}/K_m for ampicillin, compared to both the wild-type PER-2 and Arg220 mutants.

For cephalothin, cefotaxime, and ceftazidime, higher K_m values with a concomitant reduction in the turnover rates (smaller k_{cat}) in all Arg220 mutants were observed, yielding relative k_{cat}/K_m values that were slightly weaker than those for the wild-type PER-2. Moreover, for ceftazidime, only k_{cat}/K_m values could be determined, resulting in K_m values within the millimolar range and unreachable maximum velocities under the experimental conditions (data not shown). Aztreonam hydrolysis was considerably affected in all Arg220 mutants, where only K_m values were substantially modified (up to 145-fold increase in K_m values) while keeping almost invariable k_{cat} values, resulting in relative catalytic efficiencies as low as 3%.

Cefepime behaved in a different way, with smaller reductions in k_{cat}/K_m values in comparison to the wild-type PER-2 and compared to other oxyimino- β -lactams such as cefotaxime, ceftazidime, and aztreonam; only the Arg220Gly mutant displayed a strong reduction in catalytic efficiency. *In silico* models of PER-2 with cefepime (not shown) showed unfavorable interactions between Arg220 and the quaternary ammonium of

TABLE 2 (continued)

Ceftazidime			Cefepime			Aztreonam ^a		
k_{cat} (s ⁻¹)	K_m (μM)	k_{cat}/K_m (μM ⁻¹ s ⁻¹)	k_{cat} (s ⁻¹)	K_m (μM)	k_{cat}/K_m (μM ⁻¹ s ⁻¹)	k_{cat} (s ⁻¹)	K_m (μM)	k_{cat}/K_m (μM ⁻¹ s ⁻¹)
75 ± 1	105 ± 4	0.71 ± 0.04	18.6 ± 0.6	40 ± 2	0.47 ± 0.05	1.0 ± 0.1	2.4 ± 0.1	0.40 ± 0.07
ND ^b	ND	0.0266 ± 0.0003	ND	ND	0.130 ± 0.003	1.16 ± 0.04	136 ± 2	0.0085 ± 0.0005
ND	ND	0.0719 ± 0.0006	27 ± 1	103 ± 10	0.26 ± 0.05	0.75 ± 0.04	73 ± 3	0.010 ± 0.001
ND	ND	0.0655 ± 0.0008	ND	ND	0.060 ± 0.002	1.12 ± 0.06	350 ± 11	0.0032 ± 0.0003
ND	ND	0.041 ± 0.001	21 ± 2	164 ± 30	0.13 ± 0.04	0.80 ± 0.06	148 ± 7	0.0054 ± 0.0007
ND	ND	0.094 ± 0.001	18 ± 1	80 ± 9	0.22 ± 0.04	1.05 ± 0.06	181 ± 2	0.0058 ± 0.0004
ND	ND	0.0647 ± 0.0008	63 ± 6	268 ± 33	0.24 ± 0.05	0.93 ± 0.05	234 ± 5	0.0039 ± 0.0003
ND	ND	0.351 ± 0.003	117 ± 11	326 ± 43	0.36 ± 0.08	2.545 ± 0.006	13.4 ± 0.3	0.190 ± 0.004

cefepime at C-3, not present in cefotaxime, that could explain the different catalytic properties of PER-2 over cefotaxime and cefepime, at least in the Arg220Gly mutant. The β -lactamase stability of cefepime and other fourth-generation broad-spectrum cephalosporins is possibly related to a reaction scheme involving a branched pathway with a relatively stable modified acyl enzyme dependent on the nature of the C-3 leaving group (19). In PER-2, both electron-withdrawing properties and interaction between Arg220 and C-3-ammonium could therefore induce different catalytic properties over cefotaxime and cefepime. In PER-1, the Arg220Leu mutation resulted in the opposite behavior: a general increase in apparent affinity of cefotaxime, ceftazidime, and aztreonam was observed, and an increase in k_{cat}/K_m was also noticed (12).

The Thr237Ala substitution resulted in an enzyme with either lower turnover values (cephalothin and cefotaxime) or higher K_m constants (cefepime and aztreonam), giving lower catalytic efficiency values toward the cephalosporins and aztreonam compared to the wild-type PER-2. Nevertheless, the k_{cat}/K_m values remained much higher than those for Arg220-harboring mutants, which is in agreement with our previous observations suggesting a minor role of Thr237 in the overall stabilization of the active site coordination (13). In PER-1, the Thr237Ala modification yielded an enzyme with increased k_{cat}/K_m ratios for cefotaxime, ceftazidime, and aztreonam (12), this behavior being opposite to what we observed in PER-2.

It is noteworthy that the catalytic efficiencies of mutants with mutations in both Arg220 and Thr237 diminished in the same proportion toward cefotaxime and ceftazidime compared to wild-type PER-2.

Mutations at Arg220 and Thr237 do not seem to disturb the PER-2 secondary and tertiary structures globally. According to the circular dichroism (CD) and fluorescence spectra (see Fig. S1 in the supplemental material), we propose that both wild-type PER-2 and derived Arg220 and Thr237 mutants present equivalent secondary and tertiary structures. Therefore, mutations in either position might only lead to subtle local rearrangements that do not alter the overall conformation of the variants. Moreover, chemical-induced equilibrium unfolding transitions reveal that all proteins follow a similar mechanism involving, at least, the existence on an intermediate species (Fig. S1). Although quantitative differences in the thermodynamic parameters are obtained (see Table S1 in the supplemental material), the main conclusion of this approach is that all protein variants have similar stability to the wild-type protein and therefore they should be considered stable and well-folded entities.

Mutations at Arg220 and Thr237 have different outcomes in phenotypic behavior. The MIC values obtained for *Escherichia coli* Top10F' clones producing wild-type PER-2 and the derived mutants are shown in Table 3.

Overall, clavulanic acid restored partner ampicillin activity in most variants to the levels found in the recipient strain only when 10 μg/ml was used, due to the inherently high-level resistance conferred to this drug. The exception was the *E. coli* strain producing the Arg220Gly mutant, in the presence of both 1 and 10 μg/ml clavulanic

TABLE 3 MICs of selected antibiotics on recombinant clones

Plasmid harbored by <i>E. coli</i> Top10F' derivative	MIC ($\mu\text{g/ml}$) of ^a :							
	AMP	AMP-CL 1	AMP-CL 10	CEF	CTX	CAZ	FEP	AZT
No plasmid	4	4	2	8	<0.03	0.125	0.03	0.125
pK19	4	4	2	8	<0.03	0.25	0.03	0.25
pK19/PER-2 (WT)	>1,024	16	4	>1,024	128	>1,024	64	>256
pK19/PER-2 Arg220Leu	1,024	16	4	64	0.5	128	8	16
pK19/PER-2 Arg220Ser	>1,024	16	4	256	2	512	8	32
pK19/PER-2 Arg220Gly	>1,024	128	16	16	0.5	128	8	32
pK19/PER-2 Arg220His	1,024	16	4	64	1	256	8	16
pK19/PER-2 Arg220Thr	1,024	16	4	32	0.5	64	4	8
pK19/PER-2 Arg220Cys	512	16	4	64	2	64	2	16
pK19/PER-2 Thr237Ala	>1,024	16	8	512	16	>1,024	32	>256

^aAMP, ampicillin; CEF, cephalothin; CAZ, ceftazidime; CTX, cefotaxime; FEP, cefepime; AZT, aztreonam; CL, clavulanic acid. CL 1 and CL 10 correspond to 1- and 10- $\mu\text{g/ml}$ fixed concentrations of the inhibitor, respectively.

acid. For the other Arg220 mutants, the amino acid substitutions did not impact final phenotypic behavior in the presence of clavulanate, in opposition to what could be expected considering the previous findings on mutations at Arg244 in TEM β -lactamases (16). This correlated to the observed kinetic behavior of the different variants, provided that a strong reduction in the inhibition efficiency is necessary to have a phenotypic impact on the susceptibility, and only the Arg220Gly mutation, resulting in up to a 300-fold decrease in the k_{inact}/K_i value, was able to give a marked increase in the MIC of ampicillin-clavulanate (Table 1).

The MIC of cephalothin for the *E. coli* clone producing the Arg220Gly variant was reduced in at least 6 serial dilutions. The MICs of cefotaxime were reduced up to 8 serial dilutions in clones producing all the tested Arg220 variants, compared to the wild-type PER-2. For ceftazidime, even when the MICs were reduced, these values were still higher than those for other oxyimino-cephalosporins. For cefepime, the MICs were reduced at least 3 serial dilutions in *E. coli* clones producing all PER-2 mutants. For aztreonam, an up to 5-dilution decrease in the MIC was observed (Arg220Thr variant).

On the other hand, replacement of Thr237 with alanine seemed to have minor impact in the observed MICs of *E. coli* clones, which were similar to those of the *E. coli* clone producing wild-type PER-2, and only cefotaxime MIC was reduced in 3 serial dilutions compared to the wild-type producer.

Conclusions. Alterations in the hydrogen bonding network of the active site in PER-2, through modifications in such key residues as Arg220 and (to a much lesser extent) Thr237, impact not only the overall susceptibility for inactivation by mechanism-based inhibitors but also cephalosporin hydrolysis.

Mutations at Arg220 entail modifications in the catalytic activity of PER-2, and probably local perturbations in the protein, but not global conformational changes. Therefore, the apparent structural stability of the mutants suggests that these enzymes might be selected *in vivo* if the use of β -lactams/ β -lactamase inhibitors is intensified, and dissemination of $bla_{\text{PER-2}}$ genes is associated with more prevalent plasmid types. This would eventually ensure the accumulation of naturally occurring mutations that result in successful amino acid substitutions.

Our findings also reinforce the constant need for, at least, an active surveillance in those countries where PER-2 β -lactamases are still detected, as well as in others in which PER enzymes are not common. This is especially important during molecular screening of $bla_{\text{PER-2}}$ genes, as its presence could be underestimated due to the use of improper primers for its detection (i.e., the original primers used for detecting $bla_{\text{PER-1}}$ do not detect $bla_{\text{PER-2}}$ properly) or because the enzyme may be occasionally confused for other ESBLs with similar phenotypic behaviors.

MATERIALS AND METHODS

Strains and plasmids. *E. coli* TC9 is a transconjugant clone harboring the pCf587 plasmid, used as the source of the $bla_{\text{PER-2}}$ gene (11). *E. coli* Top10F' (Invitrogen, USA) and *E. coli* BL21(DE3) (Novagen, USA)

TABLE 4 List of oligonucleotide primers used to generate the *bla*_{PER-2} allelic variants and recombinant plasmids encoding the Arg220 and Thr237 PER-2 mutants

Primer name ^a	Primer sequence (5'→3') ^b	Recombinant plasmid
PER2-RxL-Fw	GAAACCACCACAGG GGCCC AGCTGTTAAAAGGCTTGTACCTGC	pK19/PER-2 Arg220Leu
PER2-RxL-Rv	GCAGGTAACAAGCCTTTTAA CA GCTG GGGCC CTGTGGTGGTTTC	
PER2-RxS-Fw	GAAACCACCACAGG GGCCC AG AG CTTAAAAGGCTTGTACCTGC	pK19/PER-2 Arg220Ser
PER2-RxS-Rv	GCAGGTAACAAGCCTTTTAA AG CTCTG GGGCC CTGTGGTGGTTTC	
PER2-RxG-Fw	GAAACCACCACAGG GGCCC AG GG CTTAAAAGGCTTGTACCTGC	pK19/PER-2 Arg220Gly
PER2-RxG-Rv	GCAGGTAACAAGCCTTTTAA AG CCTG GGGCC CTGTGGTGGTTTC	
PER2-RxH-Fw	GAAACCACCACAGG GGCCC AG CA TTTAAAAGGCTTGTACCTGC	pK19/PER-2 Arg220His
PER2-RxH-Rv	GCAGGTAACAAGCCTTTTAA AT GCTG GGGCC CTGTGGTGGTTTC	
PER2-RxT-Fw	GAAACCACCACAGG GGCCC AG AC GTTAAAAGGCTTGTACCTGC	pK19/PER-2 Arg220Thr
PER2-RxT-Rv	GCAGGTAACAAGCCTTTTAA AG CTCTG GGGCC CTGTGGTGGTTTC	
PER2-RxC-Fw	GAAACCACCACAGG GGCCC AG TG CTTAAAAGGCTTGTACCTGC	pK19/PER-2 Arg220Cys
PER2-RxC-Rv	GCAGGTAACAAGCCTTTTAA AG CACTG GGGCC CTGTGGTGGTTTC	
PER2-T237A-Fw	TAAACCGGT G CTTCGGGCGTCAGAGCAGAAAACTGC	pK19/PER-2 Thr237Ala
PER2-T237A-Rv	CTCTGACGCCGAAG C ACCGGTTTTATGCGCCACTATA	

^aFw, forward primer; Rv, reverse primer.

^bNucleotides that differ from the original sequence are shown in boldface. Restriction sites for the Apal enzyme generated by a silent mutation are underlined.

were hosts for transformation experiments. Plasmid vectors pTZ57R/T (Thermo Scientific, USA), pJET1.2/blunt (Thermo Scientific, USA), and pK19 (20) were used for routine cloning experiments. Kanamycin-resistant pET28a(+) (Novagen, Germany) was used as an overexpression vector.

Antibiotic susceptibility. MICs of β -lactams were evaluated on *E. coli* Top10F' clones producing PER-2 variants by the agar dilution method according to the Clinical and Laboratory Standards Institute (CLSI) recommendations (21). For β -lactam- β -lactamase inhibitor combinations, empirical concentrations of inhibitors were tested in order to assess their ability to protect the partner β -lactam.

Molecular biology techniques. Plasmid DNA (pCf587) was purified using the GeneJET plasmid miniprep kit (Thermo Scientific, USA). The *bla*_{PER-2} gene and the two upstream promoter regions were amplified by PCR from plasmid pCf587, using 0.6 U *Pfu* DNA polymerase (Thermo Scientific, USA) and 1 μ M PER2-BamF4 (5'-TCATGTGAGTTTGGATCCCAAGTG-3') and PER2-KpnR (5'-GAAGCGACGGTACCTAATAACTG-3') primers, containing the BamHI and KpnI restriction sites, respectively (underlined). The PCR product was first ligated in a pTZ57R/T vector (Thermo Scientific, USA); the insert was sequenced for verification of the identity of the *bla*_{PER-2} gene and generated restriction sites, as well as the absence of aberrant nucleotides. The resulting recombinant plasmid (pTZ/PER2-BK) was then digested with BamHI and KpnI, and the released insert was subsequently purified and cloned in the BamHI-KpnI sites of a pK19 vector to yield plasmid pK19/PER-2, which was used as a template to obtain mutants at Arg220 and Thr237 by a two-stage procedure based on the QuikChange site-directed mutagenesis protocol as described by Wang and Malcolm (22). The generated mutants and primers used for generating the amino acid substitutions are detailed in Table 4. The new recombinant plasmids harboring the different mutations were used to transform *E. coli* Top10F' competent cells for sequencing and antimicrobial susceptibility evaluation. After the presence of the mutations were verified by DNA sequencing, the wild-type *bla*_{PER-2} gene and the different allelic variants were amplified by PCR using 0.6 U *Pfu* DNA polymerase (Thermo Scientific, USA) and 1 μ M PER2-NdeI (5'-AGTTCATTTATATGTCAGCCCAATC-3') and PER2-SacR1 (5'-CTTTAAGAGCTCGCTTAGATAGTG-3') primers, containing the NdeI and SacI restriction sites, respectively (underlined). PCR products were cloned in the NdeI-SacI sites of a pET28a(+) vector and transformed into chemically competent *E. coli* BL21(DE3) cells upon selection in LB agar plates supplemented with 30 μ g/ml kanamycin. Final recombinant plasmids were sequenced at Macrogen, Inc. (South Korea), for nucleotide sequence verification. Nucleotide and amino acid sequence analysis was performed with NCBI (<http://www.ncbi.nlm.nih.gov/>) and ExPASy (<http://www.expasy.org/>) bioinformatics tools.

Enzyme production and purification. Overnight cultures were diluted (1/20) in 300 ml LB containing 30 μ g/ml kanamycin and grown at 37°C until they reached ca. 0.8 optical density (OD) unit ($\lambda = 600$ nm). In order to induce β -lactamase expression, 1 mM IPTG (isopropyl- β -D-thiogalactopyranoside) was added, and cultures were incubated at 18°C overnight. After centrifugation at 8,000 rpm (4°C) in a Sorvall RC-5C, cells were resuspended in buffer A (20 mM sodium phosphate buffer [pH 8.0], 0.5 M sodium chloride), and crude extracts were obtained by sonication. After clarification by centrifugation at 12,000 rpm (4°C), supernatants containing the respective fusion proteins were filtered by 0.45- and 0.22- μ m-pore-size membranes and loaded onto 1-ml HisTrap HP affinity columns (GE Healthcare Life Sciences, USA) equilibrated with buffer A; the columns were extensively washed to remove unbound proteins, and β -lactamases were eluted with a step gradient with 125 and 300 mM imidazole in buffer A (1-ml/min flow rate). Active eluted fractions were dialyzed overnight against 20 mM Tris-HCl (pH 8.0) and then against 1 \times phosphate-buffered saline (PBS) (pH 7.4). The His tag was eliminated by thrombin digestion (16 h at 22°C), using 1 U thrombin per mg protein for complete proteolysis, and removed by affinity chromatography in 1-ml HisTrap HP columns (GE Healthcare Life Sciences, USA). Protein purity was estimated as >95% by analysis on 12% SDS-PAGE gels and Coomassie blue staining, and protein concentration was determined by measuring the absorbance at 280 nm, according to the Lambert-Beer law (molar extinction coefficient for PER-2 = 33,700 M⁻¹ cm⁻¹) (23).

Steady-state kinetics. Steady-state kinetic parameters were determined using a T80 UV/visible (UV/vis) spectrophotometer (PG Instruments, Ltd., UK). Each reaction was performed in a total volume of 500 μl at 22 to 24°C in 1 \times PBS buffer. The steady-state kinetic parameters K_m and V_{max} were obtained by measuring initial rates (v_0) as described previously (24), with nonlinear least-squares fit of the data (Henri Michaelis-Menten equation [equation 1]) using GraphPad Prism 5.03 for Windows (GraphPad Software, San Diego, CA, USA):

$$v = \frac{V_{\text{max}} \times [S]}{K_m + [S]} \quad (1)$$

For low K_m values, the k_{cat} values were derived by evaluation of the complete hydrolysis time courses as described by De Meester et al. (25). For competitive inhibitors, or poor substrates (in the equations, “[S]” represents the substrate concentration), inhibition constant K_i (as K_i observed [$K_{i \text{ obs}}$]) was determined by monitoring the residual activity of the enzyme in the presence of various concentrations of the drug and 100 μM nitrocefin as the reporter substrate (11). For irreversible inhibitors, the rate constant of inactivation, k_{inact} , was measured directly by time-dependent inactivation of PER-2 in the presence of the inhibitor, using a fixed concentration of enzyme and 100 μM nitrocefin as a reporter substrate and increasing concentrations of the inhibitor. The observed rate constants for inactivation (k_{obs}) were determined by nonlinear least-squares fit of the data using OriginPro 8.0 (Northampton, MA, USA), using equation 2, as described elsewhere (26):

$$A = A_0 + v_f \times t + (v_0 - v_f) \times (1 - e^{-k_{\text{obs}} \times t}) / k_{\text{obs}} \quad (2)$$

The k_{obs} values were plotted against the inhibitor concentration, and inactivation constant k_{inact} and $K_{i \text{ obs}}$ were obtained by nonlinear fitting of equation 3 using GraphPad Prism:

$$k_{\text{obs}} = \frac{k_{\text{inact}} \times [I]}{K_{i \text{ obs}} + [I]} \quad (3)$$

In cases in which equation 3 brings a linear fitting (instead of a nonlinear fit), it was assumed that K_i values were much higher than the inhibitor concentration ($[I]$) range, for which the resulting slope is k_{inact}/K_i .

Finally, K_i was obtained from $K_{i \text{ obs}}$, taking into account substrate K_m using equation 4:

$$K_i = \frac{K_{i \text{ obs}}}{(1 + [S]) / K_m(S)} \quad (4)$$

The following extinction coefficients and wavelengths were used: ampicillin, $\Delta\epsilon_{235} = -820 \text{ M}^{-1} \text{ cm}^{-1}$; cephalothin, $\Delta\epsilon_{273} = -6,300 \text{ M}^{-1} \text{ cm}^{-1}$; ceftazidime, $\Delta\epsilon_{260} = -9,000 \text{ M}^{-1} \text{ cm}^{-1}$; cefotaxime, $\Delta\epsilon_{260} = -7,500 \text{ M}^{-1} \text{ cm}^{-1}$; cefepime, $\Delta\epsilon_{260} = -10,000 \text{ M}^{-1} \text{ cm}^{-1}$; aztreonam, $\Delta\epsilon_{318} = -750 \text{ M}^{-1} \text{ cm}^{-1}$; and nitrocefin, $\Delta\epsilon_{482} = +15,000 \text{ M}^{-1} \text{ cm}^{-1}$.

Circular dichroism. Spectra were recorded on a Jasco J-810 spectropolarimeter 810 (Jasco, Inc., Easton, MD). Data in the near-UV (250- to 320-nm) or in the far-UV (195- to 250-nm) regions were collected at 25°C using 10- or 1-mm path-length cuvettes, respectively. A scan speed of 20 nm/min with a time constant of 1 s was used for all proteins. Each spectrum was measured at least three times, and the data were averaged to minimize noise. Molar ellipticity was calculated as described elsewhere (27), using a mean residue weight value of 107.

Fluorescence measurements. Fluorescence measurements were performed at 25°C in a Jasco FP-6500 spectrofluorimeter equipped with a thermostated cell. A 3-mm-path cuvette sealed with a Teflon cap was used. The excitation wavelength was 295 nm, and emission was collected in the range 310 to 410 nm. The excitation and emission monochromator slit widths were both set at 3 nm.

Chemical denaturation. Conformational transitions were monitored as a function of denaturant concentration by measuring the change in the intrinsic fluorescence intensity of the proteins. Individual samples of protein ($\sim 10 \mu\text{M}$ final concentration) ranging in denaturant concentration from 0 to 3 M guanidinium chloride (GdmCl) were prepared by dilution of a fixed volume of a stock solution of protein in mixtures of 1 \times PBS buffer and 5 M GdmCl. Samples were analyzed after incubation for at least 1 h to ensure that the equilibrium had been reached.

Data did not fit well to a two-state unfolding transition. Therefore, the data were fitted to a three-state model with two sequential transitions and one partially folded state I. Since the three-state model may be an oversimplification and more complex equilibria may occur, the calculated curves are discussed only to illustrate general differences between the variants and are not to be taken as supportive of a particular unfolding mechanism, as proposed by Santos et al. for *Bacillus licheniformis* exo-small β -lactamase (28).

SUPPLEMENTAL MATERIAL

Supplemental material for this article may be found at <https://doi.org/10.1128/AAC.02193-16>.

SUPPLEMENTAL FILE 1, PDF file, 1.5 MB

ACKNOWLEDGMENTS

This work was supported by grants from the University of Buenos Aires (UBACyT 2014-2017 to P.P.), Consejo Nacional de Investigaciones Científicas y Técnicas (CONICET

PIP 2013-2015 to G.G.), Agencia Nacional de Promoción Científica y Tecnológica (PID 2011-0742 to G.G. and 2014-0457 to P.P.), the Fonds de la Recherche Scientifique (IISN 4.4505.09, IISN 4.4509.11, FRFC 2.4511.06F), and the University of Liège (Fonds Spéciaux, Crédit Classique, C-06/19 and C-09/75) and by a bilateral scientific agreement (V4/325C) between the Belgian Funds for Scientific Research (FRS-FNRS) to M.G. and the Consejo Nacional de Investigaciones Científicas y Técnicas (CONICET), first to G.G. and later to P.P.

M.R. is a Postdoctoral Fellow and L.C., P.P. and G.G. are researchers for the Consejo Nacional de Investigaciones Científicas y Técnicas (CONICET), Argentina.

REFERENCES

- Gutkind GO, Di Conza J, Power P, Radice M. 2013. β -Lactamase-mediated resistance: a biochemical, epidemiological and genetic overview. *Curr Pharm Des* 19:164–208. <https://doi.org/10.2174/138161213804070320>.
- Bradford PA. 2001. Extended-spectrum β -lactamases in the 21st Century: characterization, epidemiology, and detection of this important resistance threat. *Clin Microbiol Rev* 14:933–951. <https://doi.org/10.1128/CMR.14.4.933-951.2001>.
- Canton R, Morosini MI, de la Maza OM, de la Pedrosa EG. 2008. IRT and CMT β -lactamases and inhibitor resistance. *Clin Microbiol Infect* 14(Suppl 1):S53–S62. <https://doi.org/10.1111/j.1469-0691.2007.01849.x>.
- Kliebe C, Nies BA, Meyer JF, Tolxdorff-Neutzling RM, Wiedemann B. 1985. Evolution of plasmid-coded resistance to broad-spectrum cephalosporins. *Antimicrob Agents Chemother* 28:302–307. <https://doi.org/10.1128/AAC.28.2.302>.
- Queenan AM, Bush K. 2007. Carbapenemases: the versatile β -lactamases. *Clin Microbiol Rev* 20:440–458. <https://doi.org/10.1128/CMR.00001-07>.
- Lartigue MF, Poirel L, Aubert D, Nordmann P. 2006. In vitro analysis of ISEcp1B-mediated mobilization of naturally occurring β -lactamase gene *bla*_{CTX-M} of *Kluyvera ascorbata*. *Antimicrob Agents Chemother* 50:1282–1286. <https://doi.org/10.1128/AAC.50.4.1282-1286.2006>.
- Rodríguez MM, Power P, Radice M, Vay C, Famiglietti A, Galleni M, Ayala JA, Gutkind G. 2004. Chromosome-encoded CTX-M-3 from *Kluyvera ascorbata*: a possible origin of plasmid-borne CTX-M-1-derived cefotaximases. *Antimicrob Agents Chemother* 48:4895–4897. <https://doi.org/10.1128/AAC.48.12.4895-4897.2004>.
- Nordmann P, Ronco E, Naas T, Duport C, Michel-Briand Y, Labia R. 1993. Characterization of a novel extended-spectrum β -lactamase from *Pseudomonas aeruginosa*. *Antimicrob Agents Chemother* 37:962–969. <https://doi.org/10.1128/AAC.37.5.962>.
- Quinteros M, Radice M, Gardella N, Rodríguez MM, Costa N, Korbenfeld D, Couto E, Gutkind G, Microbiology Study Group. 2003. Extended-spectrum β -lactamases in *Enterobacteriaceae* in Buenos Aires, Argentina, public hospitals. *Antimicrob Agents Chemother* 47:2864–2869. <https://doi.org/10.1128/AAC.47.9.2864-2867.2003>.
- Vignoli R, Varela G, Mota MI, Cordeiro NF, Power P, Ingold E, Gadea P, Sirok A, Schelotto F, Ayala JA, Gutkind G. 2005. Enteropathogenic *Escherichia coli* strains carrying genes encoding the PER-2 and TEM-116 extended-spectrum β -lactamases isolated from children with diarrhea in Uruguay. *J Clin Microbiol* 43:2940–2943. <https://doi.org/10.1128/JCM.43.6.2940-2943.2005>.
- Power P, Di Conza J, Rodríguez MM, Ghiglione B, Ayala JA, Casellas JM, Radice M, Gutkind G. 2007. Biochemical characterization of PER-2 and genetic environment of *bla*_{PER-2}. *Antimicrob Agents Chemother* 51:2359–2365. <https://doi.org/10.1128/AAC.01395-06>.
- Bouthors AT, Delette J, Mugnier P, Jarlier V, Sougakoff W. 1999. Site-directed mutagenesis of residues 164, 170, 171, 179, 220, 237 and 242 in PER-1 β -lactamase hydrolysing expanded-spectrum cephalosporins. *Protein Eng* 12:313–318. <https://doi.org/10.1093/protein/12.4.313>.
- Ruggiero M, Kerff F, Herman R, Sapunaric F, Galleni M, Gutkind G, Charlier P, Sauvage E, Power P. 2014. Crystal structure of the extended-spectrum β -lactamase PER-2 and insights into the role of specific residues in the interaction with β -lactams and β -lactamase inhibitors. *Antimicrob Agents Chemother* 58:5994–6002. <https://doi.org/10.1128/AAC.00089-14>.
- Papp-Wallace KM, Taracila MA, Smith KM, Xu Y, Bonomo RA. 2012. Understanding the molecular determinants of substrate and inhibitor specificity in the carbapenemase KPC-2: exploring the roles of Arg220 and Glu276. *Antimicrob Agents Chemother* 56:4428–4438. <https://doi.org/10.1128/AAC.05769-11>.
- Perez-Llarena FJ, Cartelle M, Mallo S, Beceiro A, Villanueva R, Romero A, Bonnet R, Bou G. 2008. Structure-function studies of arginine at position 276 in CTX-M β -lactamases. *J Antimicrob Chemother* 61:792–797. <https://doi.org/10.1093/jac/dkn031>.
- Bret L, Chaibi EB, Chanal-Claris C, Sirot D, Labia R, Sirot J. 1997. Inhibitor-resistant TEM (IRT) β -lactamases with different substitutions at position 244. *Antimicrob Agents Chemother* 41:2547–2549.
- Thomson JM, Distler AM, Prati F, Bonomo RA. 2006. Probing active site chemistry in SHV β -lactamase variants at Ambler position 244. Understanding unique properties of inhibitor resistance. *J Biol Chem* 281:26734–26744. <https://doi.org/10.1074/jbc.M603222200>.
- Bonomo RA, Rice LB. 1999. Inhibitor resistant class A β -lactamases. *Front Biosci* 4:e34–e41. <https://doi.org/10.2741/Bonomo/10.2741/A477>.
- Laws A, Page M. 1996. The chemistry and structure-activity relationships of C3-quaternary ammonium cephem antibiotics. *J Chemother* 8(Suppl 2):S7–S22.
- Pridmore RD. 1987. New and versatile cloning vectors with kanamycin-resistance marker. *Gene* 56:309–312. [https://doi.org/10.1016/0378-1119\(87\)90149-1](https://doi.org/10.1016/0378-1119(87)90149-1).
- Clinical and Laboratory Standards Institute. 2016. Methods for dilution antimicrobial susceptibility tests for bacteria that grow aerobically, 10th ed. Approved standard M7-A10, vol 36. Clinical and Laboratory Standards Institute, Wayne, PA.
- Wang W, Malcolm BA. 1999. Two-stage PCR protocol allowing introduction of multiple mutations, deletions and insertions using QuikChange site-directed mutagenesis. *Biotechniques* 26:680–682.
- Layne E. 1957. Spectrophotometric and turbidimetric methods for measuring proteins. *Methods Enzymol* 3:447–455. [https://doi.org/10.1016/S0076-6879\(57\)03413-8](https://doi.org/10.1016/S0076-6879(57)03413-8).
- Segel IH. 1975. Enzyme kinetics, behavior and analysis of rapid equilibrium and steady-state enzyme systems. John Wiley & Sons, Inc, New York, NY.
- De Meester F, Joris B, Reckinger G, Bellefroid-Bourguignon C, Frere JM, Waley SG. 1987. Automated analysis of enzyme inactivation phenomena. Application to β -lactamases and DD-peptidases. *Biochem Pharmacol* 36:2393–2403.
- Papp-Wallace KM, Bethel CR, Distler AM, Kasuboski C, Taracila M, Bonomo RA. 2010. Inhibitor resistance in the KPC-2 β -lactamase, a preeminent property of this class A β -lactamase. *Antimicrob Agents Chemother* 54:890–897. <https://doi.org/10.1128/AAC.00693-09>.
- Schmidt FX. 1989. Spectral methods of characterizing protein conformation and conformational changes, p 251–285. *In* Creighton TE (ed), Protein structure: a practical approach. IRL Press, New York, NY.
- Santos J, Rizzo VA, Sica MP, Ermacora MR. 2007. Effects of serine-to-cysteine mutations on β -lactamase folding. *Biophys J* 93:1707–1718. <https://doi.org/10.1529/biophysj.106.103804>.